

# A free-boundary MHD code for axisymmetric equilibrium configurations.

G. F. Torija-Daza<sup>1</sup>, J. M. Reynolds-Barredo<sup>1</sup>, R. Sánchez<sup>1</sup>

<sup>1</sup> *Universidad Carlos III de Madrid (UC3M), Madrid, Spain*

## Ideal MHD equilibrium in tokamaks.

Ideal 2D MHD equilibria are traditionally calculated in tokamaks under the assumption of axisymmetry and negligible plasma flows, since the problem is then reduced to solving one elliptic equation (Grad-Shafranov's) for the magnetic poloidal flux function,  $\psi$ . Toroidal axisymmetry usually remains a good approximation in most experimental situations, but the existence of macroscopic plasma flows is often not satisfied. Additionally, the consideration of plasma flows in the 2D MHD equilibrium calculation, however, significantly complicates the problem.

Nonetheless, the calculation of MHD equilibria is routinely required in many contexts in magnetically confined fusion plasmas, starting at the initial phases of the design of a confining magnetic configuration and continuing during the interpretation of multiple diagnostic systems during their operation. For instance, when assessing the consequences of adding or removing elements to/from an existing tokamak, or when making changes in its configuration. Therefore, the precise knowledge of the plasma equilibrium is maybe important is when significant poloidal and/or toroidal flows are established.

## From fix-boundary to free-boundary.

A common element to the codes that manage to deal with all this complexity [1, 2] is that they often assume a fixed plasma boundary at which the value of  $\psi$  is known and assigned from input. This approach is usually referred to as a "fixed-boundary" equilibrium solution and calculations are then restricted to the plasma region. In many cases, this is a reasonable approach since the approximate shape of the plasma edge might be experimentally available.

There are situations, however, in which the shape of the plasma may not be known in advance. Or, more interestingly, one could perhaps like to quantify how the shape of the plasma edge changes under controlled variations of discharge parameters in the presence of plasma flows (see Fig. 1). These could be the case, for instance, while investigating the consequences of

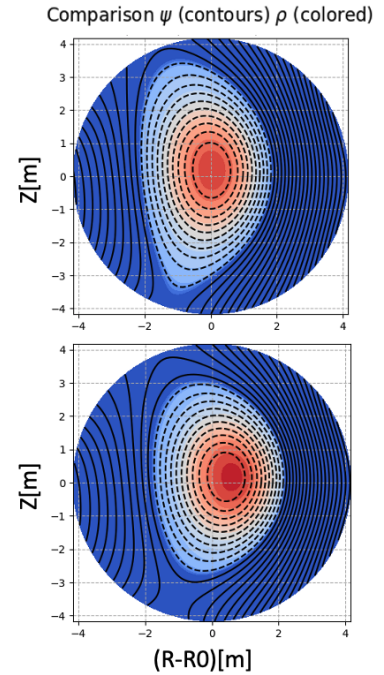


Figure 1: Variation of magnetic and density surfaces in the equilibrium of an ITER baseline configuration. Static case (up) vs high flow case (down) for profile ( $gf$ ) with scaling factor  $M_{\text{tor}} = 0.8$ .

adding new elements to, or changing the nominal current density values of an existing coil configuration. A different type of code is then needed, one in which the shape of the plasma edge is not prescribed a priori, being instead free to adapt to what the force-balance equations dictate.

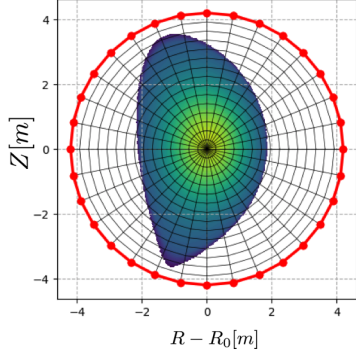


Figure 2: 2D computational domain used to solve the GSB system.

Various free-plasma-boundary solvers are available for ideal static MHD equilibria, both for tokamaks and stellarators. In this paper, we rely on this expertise to build a code that can produce free-plasma-boundary solutions of equilibria with flows for an arbitrarily complex set of external coils.

### Grad-Shafranov-Bernoulli system (GSB).

This is the most common resource in the context of axis-symmetric ideal MHD equilibrium with flows. Among all the derivation versions, the most popular GS equation is probably Hameiri's[3]. Using cylindrical coordinates  $(R, \phi, Z)$  it can be written as

$$\frac{1}{\mu_0} \nabla \cdot \left( \frac{(1 - M_{p,A}^2)}{R^2} \nabla \psi \right) = -\frac{B_\phi}{\mu_0 R} K'(\psi) - (\mathbf{v} \cdot \mathbf{B}) \chi'(\psi) - \rho H'(\psi) - R \rho v_\phi \Phi''(\psi) + \frac{\rho^\gamma}{\gamma - 1} S'(\psi) \quad (1)$$

The number of free functions to prescribe is also increased from two to five ( $K, \chi, H, \Phi$  and  $S$ ). Magnitudes and constants have been assigned as usual: velocity of the flow  $\mathbf{v}$ , density  $\rho$ , magnetic field  $B$  and the vacuum permeability  $\mu_0$ . Adiabatic index parameter,  $\gamma$ , is set to  $5/3$ . This second order PDE keeps its elliptic nature meanwhile the Alfvénic Mach number  $M_{p,A}(\psi, R)$  is less than 1, and the present work is holding this regime for all the calculations in it. Due to the nonlinear essence of the equation, other equilibrium equation is added to the solver: a version of the Bernoulli equation adapted for the current problem.

$$\frac{1}{2} \left( \frac{|\mathbf{B}|}{\rho} \chi(\psi) \right)^2 - \frac{1}{2} (R \Phi'(\psi))^2 + \frac{\gamma \rho^{\gamma-1}}{\gamma - 1} S(\psi) = H(\psi) \quad (2)$$

### The coupled free-boundary code.

Grad-Shafranov-Bernoulli system that has to be solved iteratively: First, equation (2) for density and then, equation (1) for the stream function  $\psi$  until any usual convergence criteria is fulfilled.

The code uses an eulerian frame of toroidal coordinates  $(r, \theta, \zeta)$  as it is illustrated in the example Fig. 2. Angular dependencies ( $\theta$ ) are treated with pseudo-spectral methods and second-order finite differences are applied to the radial dimension,  $r$ . The major radius of the geometri-

cal torus,  $R_0$ , is close but may not coincide with the magnetic axis. All of this leads to very good convergence properties for the residual net force, that decreases quadratically with the number of radial points,  $M_r$ , and exponentially with the number of poloidal modes,  $N_\theta$ . In addition to that, our choice of coordinates allows us to an easier interaction with the VMEC code.

As a fix-boundary condition states, a circular surface with an arbitrary minor radius  $r = r_b$  (in red in Fig. 2) and the boundary condition,  $\psi(r_b, \theta) = \psi_b(\theta)$ , must be provided by the user to match the problem of interest. But, it is updating the computational boundary what let the code to be recognized as free-boundary. Therefore, once the value of  $\psi^{(j=1)}(r, \theta)$  has been calculated by the GSB system solver, the code starts a new outer iteration in which it recalculates the plasma current contribution, updates the boundary condition to  $\psi^{(j=2)}(r = r_b, \theta)$  and calls the GSB solver again to find an updated  $\psi^{(j=2)}(r, \theta)$ , consistent with the updated boundary condition.

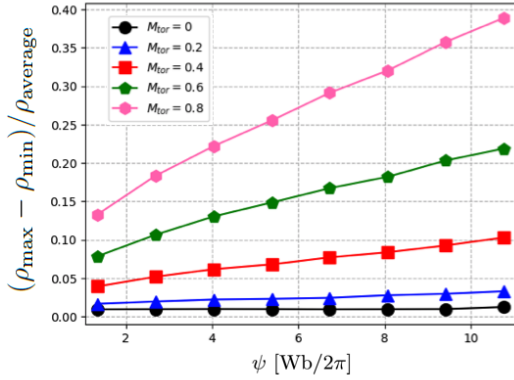


Figure 4: Variation of plasma density along various magnetic surfaces calculated for the various scaling factors  $M_{tor}$  using "(gf)" Mach number profile.

vector potential  $\mathbf{A}$  created by the plasma current density [5].

### Examples of free-plasma-boundary capabilities of the code.

As an example, an ITER equilibrium has been studied deliberately with purely toroidal flows, although our GSB code can also handle poloidal flows. The reason is that toroidal runs are faster to run, allow for a more efficient debugging and illustrate the code capabilities equally well. In order to showcasing the capabilities of the free-boundary code, we apply a set of different

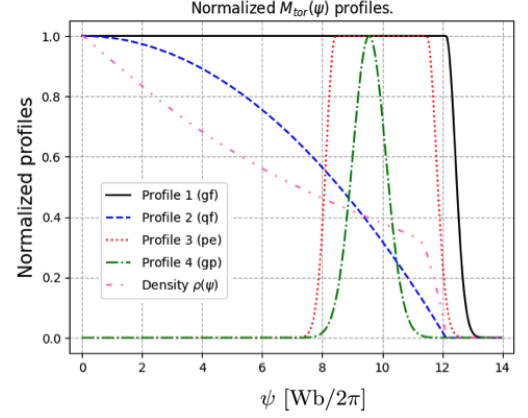
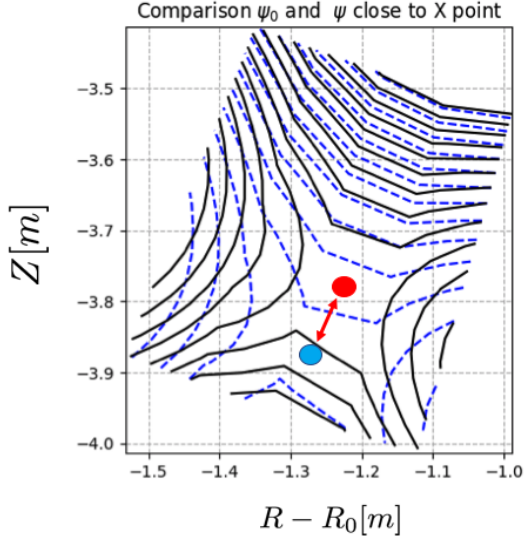


Figure 3: Normalized toroidal sonic Mach number profiles.

In order to perform this update, the contribution from the external coils must be known a priori. This calculation is carried out by the MAKEGRID code, that uses the Biot-Savart law to evaluate the contribution of each coil segment to an arbitrary selection of points on a  $R - Z$  grid. Then, the computed vacuum field let the value of  $\psi$  in the boundary to be obtained straightforward. In regards to the contribution from the plasma current, a different approach is followed. From previous experience with the SIESTA code [4], it turns out that the most numerically efficient way is to calculate the magnetic

normalized flow profiles (Fig. 3) with different intensities (controlled by a subsonic scaling factor  $M_{\text{tor}} < 1$ ) to the ITER baseline equilibrium.



**Figure 5:** Displacement of the X-point for the "(gf)" profile with scaling factor  $M_{\text{tor}} = 0.4$  relative to the position in the initial guess (dashed blue).

## Conclusions and future work.

A fixed-boundary solver for GSB system have been successfully coupled to a scheme, initially developed for the calculation of static MHD equilibria in stellarators, to enable it to efficiently compute free-plasma-boundary 2D equilibria.

The development of the code that uses generalized coordinates and a similar study including poloidal flows are currently underway.

## References

- [1] A.J.C. Beliën, Mikhail A. Bochev, J.P. Goedbloed, B. van der Holst, and R. Keppens. *Journal of computational physics*, 182(1):91–117, 2002.
- [2] L. Guazzotto, R. Betti, J. Manickam, and S. Kaye. *Physics of Plasmas*, 11(2):604–614, 2004.
- [3] Eliezer Hameiri. *The Physics of Fluids*, 26(1):230–237, 1983.
- [4] H. Peraza-Rodríguez, J. M. Reynolds-Barredo, R. Sanchez, J. Geiger, V. Tribaldos, S. P. Hirshman, and M. Cianciosa. *Physics of Plasmas*, 24(8):082516, 2017.
- [5] J.M. Reynolds-Barredo, H. Peraza-Rodríguez, R. Sanchez, and V. Tribaldos. *Journal of Computational Physics*, 406:109214, 2020.

First expected consequence in the presence of plasma flows is that the increment of  $M_{\text{tor}}$  makes the density not to be a surface quantity anymore (Fig. 4). In addition to that, the code opens the possibility of quantifying important features such as the shape of the plasma edge, the plasma confining volume and the position of the magnetic axis, density maximum or even the X-point, among others. It is worth to note that, although shifts of the maximum density are also observable and quantifiable in fixed-boundary runs, significant inaccuracies might occur if the plasma flow happens to deform the plasma boundary significantly with respect to the fixed boundary assumed. Some examples are illustrated in Fig. 5 and Fig. 6.

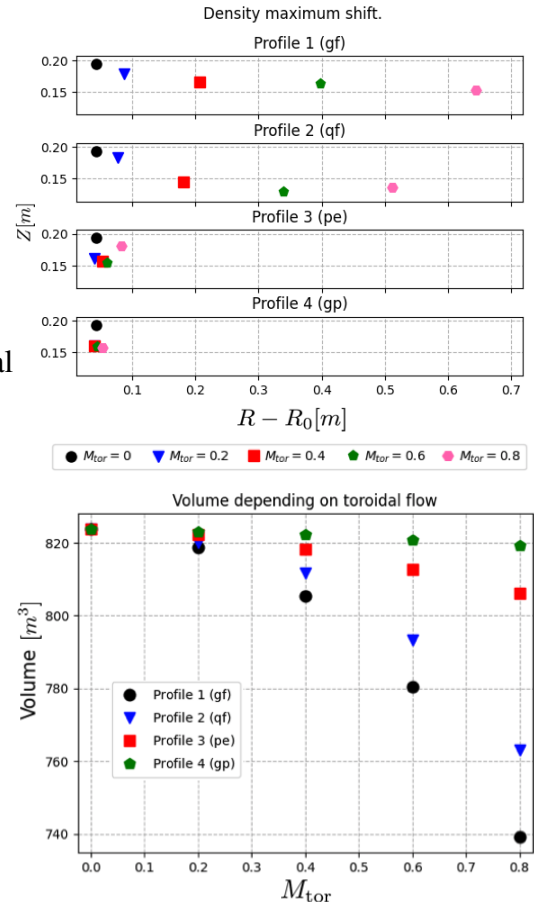


**Figure 6:** Displacement of the density maximum (up) and change in the plasma volume (down) depending on the different profiles defined in Fig. 3 and the value of the scaling factor  $M_{\text{tor}}$ .